Addressing Barriers to Efficient Renewable Integration

Grant Number: G00865

Proceedings of ECCE, 11-15 Oct 2020

Comparative Analysis of Flexible Power Point Tracking Algorithms in Photovoltaic Systems

Hossein Dehghani Tafti,
Georgios Konstantinou
Christopher D Townsend,
Glen G. Farivar,
Salvador Ceballos,
Josep Pou,
John E. Fletcher

Please visit the following websites for more information:

- Project summary: https://arena.gov.au/projects/addressing-barriers-efficient-renewable-integration
- Inverter bench testing: http://pvinverters.ee.unsw.edu.au

Comparative Analysis of Flexible Power Point Tracking Algorithms in Photovoltaic Systems

Hossein Dehghani Tafti[1*], Georgios Konstantinou[1], Christopher D Townsend[2], Glen G. Farivar[3], Salvador Ceballos[4], Josep Pou[5] and John E. Fletcher[1].
[1]School of Electrical Engineering and Telecommunications, University of New South Wales, Australia.
[2]School of Electrical, Electronic and Computer Engineering, University of Western Australia, Australia.
[3]Energy Research Institute, Nanayang Technological University, Singapore.
[4]Tecnalia, Basque Research and Technology Alliance (BRTA), Derio, Spain.
[5]School of Electrical and Electronic Engineering, Nanayang Technological University, Singapore.
[*]hossein002@e.ntu.edu.sg

***Abstract*—A significant quantity of flexible power point tracking (FPPT) algorithms has been recently proposed in the literature to provide various grid support functionalities in photovoltaic (PV) systems. These algorithms aim to regulate the PV power to a specific value, imposed by grid codes and according to operational conditions. To obtain a fair comparison between several FPPT algorithms, each algorithm must be designed with its optimum parameter values. The main contribution of this paper is to provide a detailed analysis of the effect of various parameters of three FPPT algorithms on their transient or steady-state performance. The results of this analysis are used to obtain an optimum tuning of the parameters of each algorithm to attain an enhanced performance in both transient and steady-state operating conditions. Finally, the performance of these algorithms is compared using simulation and an experimental laboratory systems.**

***Index Terms*—Active power control, flexible power point tracking, photovoltaic systems, sensitivity analysis.**

I. Introduction

To maintain the stability and quality of the power system under the high penetration of renewable energy resources, power system operators continually update the grid connection requirements and functionalities, including those for photovoltaic (PV) systems [1]. The conventional maximum power point tracking (MPPT) algorithms fail to provide these new functionalities for PV systems. Accordingly, flexible power point tracking (FPPT) algorithms are developed [2], which regulate the output power of the PV system to a desired reference value p_{fpp} (see Fig. 1(a)), calculated from an upper-level controller, based on the grid operating conditions, grid code requirements and power/current ratings of the grid-connected inverter [3], [4]. If the power reference p_{fpp} is smaller than the maximum available power, the operation point of the PV string moves to the right- or left-side of the maximum power point (MPP), i.e., $\mathrm{FPP_R}$ or $\mathrm{FPP_L}$ in Fig. 1(a). Moreover, if the available power from the PV string is smaller than the power reference, it extracts the maximum available power by operating the system at MPP_2.

The overall control scheme of a two-stage PV system (illustrated in Fig. 1(b)) consists of two main blocks, namely "PV Voltage Reference Calculation" and "PV Voltage Control" blocks. Accordingly, available FPPT algorithms in the literature can be divided into two types: I) Algorithms that modify the "PV Voltage Control" block of the power converter to obtain FPPT functionality [5], [6]. In these solutions, the "PV Voltage Reference Calculation" block is kept as a conventional MPPT algorithm. II) Algorithms with direct calculation of the PV voltage reference based on the desired power reference. In these algorithms an FPPT strategy is directly implemented in the "PV Voltage Reference Calculation" block. This FPPT algorithm calculates the PV voltage reference according to the power reference p_{fpp} in Fig. 1(a) [7], [8]. Then, this voltage reference $v_{pv\text{-}ref}$ is fed into the "PV Voltage Control" block which is not modified and remains as any conventional solution. Based on the detailed analysis in [2], the second type of the FPPT algorithms have more advantages, i.e., simpler design and fast dynamic response, compared to the first type of the algorithms. Accordingly, the second type of the FPPT algorithms are studied in this paper.

Each FPPT algorithm has several design parameters. The use of optimum design parameters for each algorithm is necessary to obtain a fair comparison between them, however, due to the nonlinear nature of the system, finding the optimum value of design parameters is challenging. The main contribution of this paper is to optimize the design parameters of each FPPT algorithm,

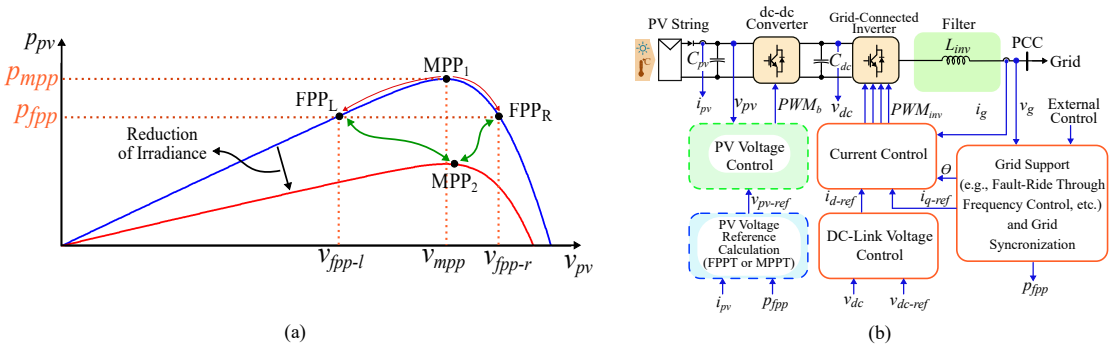

Fig. 1. (a) Principles of FPPT operation, and (B) circuit topology and overall control overview of the two-stage PV system.

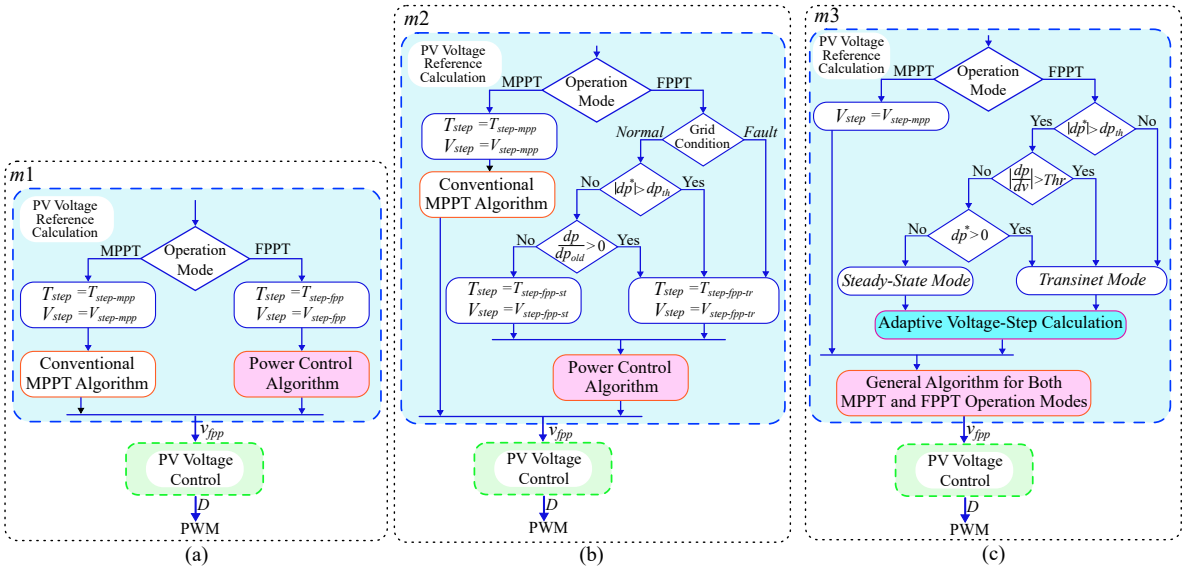

Fig. 2. Overview of various FPPT algorithms: (a) Method 1 (*m*1) - proposed algorithms in [8], [9] with constant voltage-step values, (b) proposed algorithm in [3] with different voltage-step values during transient and steady-state operation modes, and (c) Method 3 (*m*3) - FPPT algorithm with an adaptive voltage-step calculation [10].

based on the detailed analysis of the effect of the parameters of each algorithm. A comprehensive analysis on three FPPT algorithms from the Type II of FPPT algorithms, mentioned above, is provided. The proposed analysis shows the effect of each design parameter on the transient and steady-state performance of the algorithm. The results of this analysis are used to tune the parameters to minimize the overall tracking error of each algorithm. A simulation system is used to evaluate and compare the performance of these algorithms under their optimum design. The performance of these algorithms is also compared experimentally under fast changes of the irradiance. Accordingly, the main contributions of this paper can be summarized as:

- A comprehensive study of the effect of the parameters of various FPPT algorithms on their transient and steady-state performance
- Optimum tuning of the design parameters of each algorithm to enhance the performance in both steady-state and transient operating conditions
- Experimental and simulation comparison of the performance of various FPPT algorithms with optimum design.

II. Overview of FPPT Algorithms

An overview of the three FPPT algorithms is illustrated in Fig. 2. In this section, a brief explanation of their control strategy is provided.

Method 1 (m1): The algorithms in [8], [9] divide the operation modes into the MPPT and FPPT operation modes (Fig. 2(b)). During the MPPT control, a conventional MPPT algorithm, e.g., perturb and observe (P&O), is implemented to calculate the PV voltage reference v_{mpp}, corresponding to the maximum available

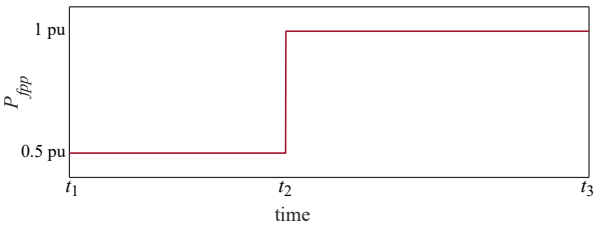

Fig. 3. The implemented step-change in the PV power reference in the analysis of various FPPT algorithms.

power. During the FPPT operation, a power control algorithm is implemented to calculate the voltage reference v_{fpp} corresponding to the PV power reference p_{fpp}. A constant voltage-step $V_{step-fpp}$ is used during all operation conditions of the FPPT control. This algorithm is flexible to move the operating point to the right- or left-side of the MPP in Fig. 1(a), however only the operation in the left-side of the MPP is studied in this paper.

Method 2 (*m*2)*:* An algorithm for the calculation of the voltage-step, based on the operational condition of the PV system (i.e. transient or steady-state), was introduced in [3] (Fig. 2(b)). During the FPPT operation, if the grid is under the *Fault* condition, a relatively large voltage-step $V_{step\text{-}fpp\text{-}tr}$ is chosen in order to enhance the transient response. Under the *Normal* operation, the difference between the amplitude of the power reference p_{fpp} and p_{pv}, calculated as $\mid dp^* \mid = \mid p_{fpp} - p_{pv} \mid$, is compared with its threshold value dp_{th}. In this way, the operation mode is divided into steady-state or transient modes. Furthermore, a hysteresis controller is implemented to use a large voltage-step $V_{step\text{-}fpp\text{-}tr}$ under transients, while a relatively small voltage step $V_{step\text{-}fpp\text{-}st}$ is used during the steady-state operation.

Method 3 (*m*3)*:* A general algorithm for flexible power tracking in PV systems was introduced in [10] (Fig. 2(c)). One general voltage reference calculation algorithm is implemented, which is able to calculate the voltage reference in both MPPT and FPPT operation modes. The main advantage of this algorithm, compared to *m*2, is the use of a fixed time-step for all operation modes. This feature reduces the implementation complexity, as well as facilitates the tuning process for controller parameters. In spite of using a fixed time-step, this algorithm uses an adaptive voltage step calculation algorithm in adjusting the voltage step to the operating point and operational condition of the PV system. More details of this algorithm can be found in [10]. This algorithm is also flexible to move the operating point to the right- or left-side of the MPP in Fig. 1(a).

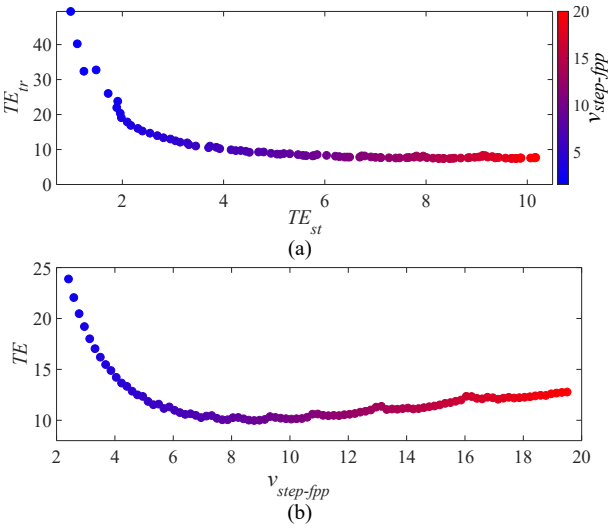

Fig. 4. Analysis of effect of change of $v_{step\text{-}fpp}$ on various tracking error values in *m*1: (a) Effect of $v_{step\text{-}fpp}$ on steady-state and transient tracking error values, and (b) effect of $v_{step\text{-}fpp}$ on overall tracking error.

III. Analysis of the Effect of Parameters in FPPT Algorithms

The proposed sensitivity analysis of the FPPT algorithms is implemented on a $1.1\,\mathrm{kW}$ two-stage PV system, shown in Fig. 1(a). The parameters of the simulation system are set similar to the parameters of the scaled-down experimental setup, which will be presented in Section IV. In order to analyze the performance of the algorithms, the following case study is implemented, as shown in Fig. 3. At the beginning, the irradiance is kept as $1000\,\mathrm{W/m^2}$ and the power reference is $p_{fpp} = 0.5\,\mathrm{p.u}$ before t_2. All the algorithms operate at steady-state condition between t_1 and t_2. Accordingly, the steady-state tracking error TE_{ss} is calculated in the following manner:

$$TE_{st} = \frac{\int_{t_1}^{t_2} \mid p_{pv} - p_{fpp} \mid}{\int_{t_1}^{t_2} \mid p_{pv} \mid} \times 100\,\%. \qquad (1)$$

In order to evaluate the transient performance of the algorithms, a step-change of the power reference from $p_{fpp} = 0.5\,\mathrm{p.u}$ to $p_{fpp} = 1\,\mathrm{p.u}$ occurs at t_2. The transient tracking error TE_{tr} is calculated between t_2 and t_3, during which that all the algorithms reach the new steady-state condition. The overall tracking error TE is defined, as follows, which is used as the optimization parameter for the calculation of the design parameters of the FPPT algorithms.

$$TE = \sqrt{\alpha.TE_{st}^2 + \beta.TE_{tr}^2}, \qquad (2)$$

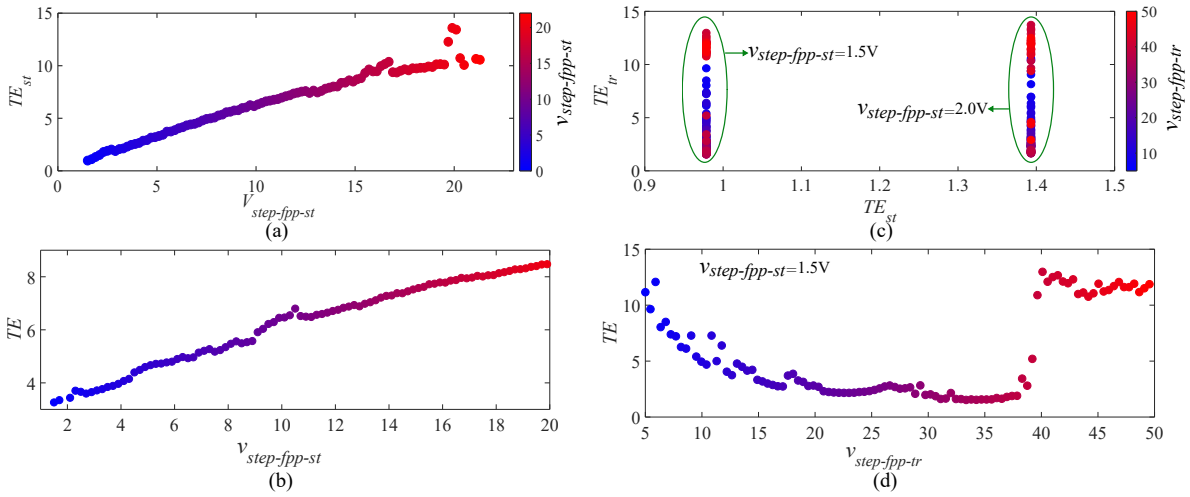

Fig. 5. Analysis of effect of change of $v_{step\text{-}fpp}$ on various tracking error values in *m*2: (a) Effect of $v_{step\text{-}fpp\text{-}st}$ on the steady-state error, (b) effect of $v_{step\text{-}fpp\text{-}st}$ on the overall tracking error, (c) effect of $v_{step\text{-}fpp\text{-}tr}$ on the steady-state and transient errors, and (d) effect of $v_{step\text{-}fpp\text{-}tr}$ on the overall tracking error.

in which, α and β are the weighting factors to adjust the significance of steady-state or transient errors on the overall tracking error. In this study, the optimum operation of an algorithm is when both the transient and steady-state error values are minimized, which means $\alpha = 1$ and $\beta = 1$.

The analysis of the effect of voltage step $V_{step\text{-}fpp}$ on various tracking error values of algorithm *m*1 is illustrated in Fig. 4. As illustrated in Fig. 2(a), the main design variable for this algorithm are time- and voltage-step of the FPPT algorithm, i.e., $T_{step}$and V_{step}. It is clear that the value of T_{step} should be chosen as small as possible in order to achieve fast transient response for the FPPT operation. It should be noted that the minimum value of T_{step} is limited by the voltage controller response. It is seen from Fig. 4(a) that larger values of $V_{step\text{-}fpp}$ results in smaller values of transient tracking error TE_{tr}, while it increases the steady-state tracking error TE_{st}. Therefore, there is a trade off between the transient and steady state tracking errors. Accordingly, the optimum value of $V_{step\text{-}fpp}$ is selected based on the overall tracking error TE, as depicted in Fig. 4(b).

The algorithm *m*2 has two main design parameters, i.e., steady state voltage step $V_{step\text{-}fpp\text{-}st}$ and transient voltage step$V_{step\text{-}fpp\text{-}tr}$, as depicted in Fig. 2(b). Initially, the value of $V_{step\text{-}fpp\text{-}st}$ should be optimized in order to minimize TE_{st}. The effect of the change of $V_{step\text{-}fpp\text{-}st}$ on TE_{st} is depicted in Fig. 5(a). It is seen that increasing the steady state voltage step results in an increased TE_{st}. As a result, the minimum possible value of the voltage step is chosen for $V_{step\text{-}fpp\text{-}st}$, which is 1.5 V in this study. Subsequently, the effect of $V_{step\text{-}fpp\text{-}tr}$ on both TE_{st} and TE_{tr} is illustrated in Fig. 5(c). Accordingly, the optimum value of $V_{step\text{-}fpp\text{-}tr}$ can be obtained based on the overall tracking error, shown in Fig. 5(d). Similarly, the results of the analysis for algorithm *m*3 are shown in Fig. 6. It should be noted that K_1 and K_2 are the design parameters and the detailed information about them can be found in [10].

The performance of the algorithms with their optimum design parameters is evaluated through simulations and results are compared in Fig. 7. It is seen that the algorithm *m*3 with adaptive voltage step calculation results in smaller tracking error compared to the other algorithms.

IV. Experimental Results

A scaled-down 1.1 kW two-stage PV system, as shown in Fig. 1(b), is implemented experimentally to compare the dynamic and steady-state performance of the investigated FPPT algorithms. The PV panel is simulated by using a Chroma 62000H-S solar array simulator, and the grid is emulated with a Cinergia grid emulator. IMPERIX H-bridge modules are used to build the two-stage PV system and the controller is implemented using the B-BOX RCP control platform from IMPERIX. The design parameters of each FPPT algorithm are set as the optimum values, calculated based on the analysis in the previous section.

The performance of investigated algorithms is verified and compared under a fast change of the irradiance and results are demonstrated in Fig. 8. The irradiance increases from 300 $\mathrm{W/m^2}$ to 1000 $\mathrm{W/m^2}$ in the period between $t = 5\,\mathrm{s}$ and $t = 10\,\mathrm{s}$, and decreases

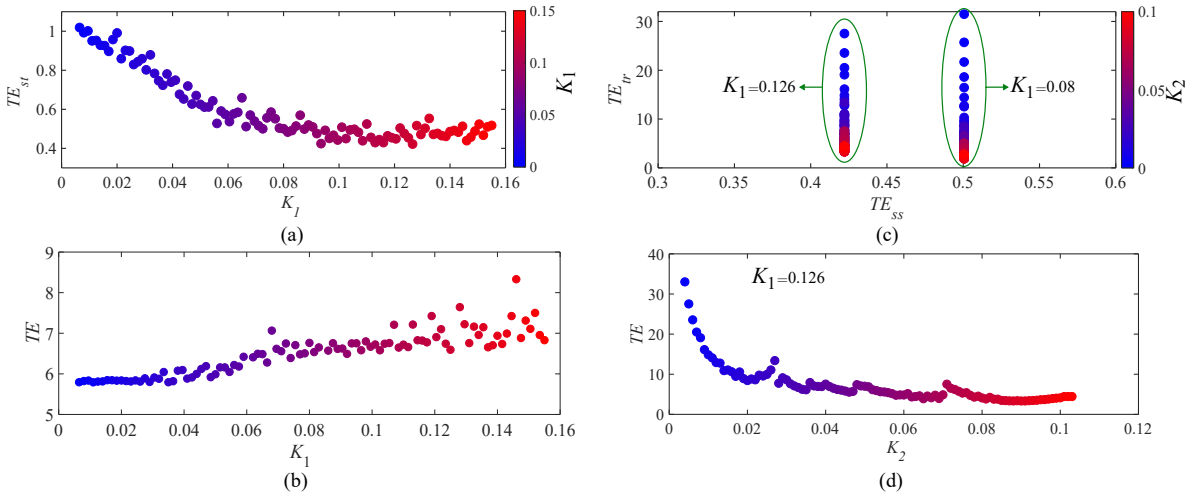

Fig. 6. Analysis of effect of change of K_1 and K_2 on various tracking error values in $m3$: (a) Effect of K_1 on the steady-state error, (b) effect of K_1 on the overall tracking error, (c) effect of K_2 on the steady-state and transient errors, and (d) effect of K_2 on the overall tracking error.

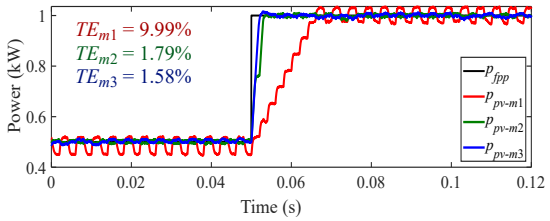

Fig. 7. Comparison of the performance of various FPPT algorithms under their optimum operation design.

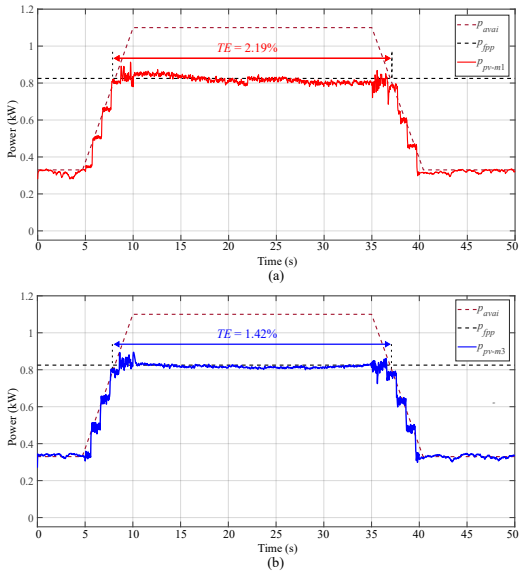

Fig. 8. Experimental performance comparison of various FPPT algorithms under fast changes of irradiance - PV power and its references for algorithms (*Irr* - irradiance): (a) $m1$, and (d) $m3$.

from $1000\,\mathrm{W/m^2}$ to $300\,\mathrm{W/m^2}$ in the period between $t = 35\,\mathrm{s}$ and $t = 40\,\mathrm{s}$. The power reference is set as 75% of the maximum available power of the PV string. The overall tracking error is calculated for $m1$ and $m3$ and is depicted in the corresponding sub-figure in Fig. 8. It is seen that the tracking error for $m3$ is the smallest among all the algorithms. This is achieved due to the adaptive calculation of the voltage step in this algorithm, which enables fast transient response under irradiance changes. It also adjusts the voltage step based on the operation point of the PV string that results in smaller steady-state tracking errors with lower power oscillations.

V. Conclusion

An overview of three FPPT algorithms has been presented in this paper. A short description of the algorithms has been provided, while an analysis of the effect of design parameters of each algorithm on the transient and steady-state performance of each algorithm has been delivered. The experimental comparison between the FPPT algorithms with optimum tuned parameters reveals that the FPPT algorithm with adaptive calculation of the voltage step provides better performance.

VI. Acknowledgment

This work was partially supported by the Singapore Ministry of Education Academic Research Fund Tier 1 under Grant No: 2019-T1-001-168 (RG 80/19) and by the Australian Renewable Energy Agency (ARENA) under the project ‘Addressing Barriers to Efficient Renewable Integration’, Grant No: G00865.

REFERENCES

[1] "IEEE standard for interconnection and interoperability of distributed energy resources with associated electric power systems interfaces," *IEEE Std 1547-2018 (Revision of IEEE Std 1547-2003)*, Apr. 2018.

[2] H. D. Tafti, G. Konstantinou, C. D. Townsend, G. Farivar, A. Sangwongwanich, Y. Yang, J. Pou, , and F. Blaabjerg, "Extended functionalities of photovoltaic systems with flexible power point tracking: Recent advances," *IEEE Trans. Power Electron.*, vol. PP., pp. 1–14, Jan. 2020.

[3] H. D. Tafti, A. I. Maswood, G. Konstantinou, J. Pou, and F. Blaabjerg, "A general constant power generation algorithm for photovoltaic systems," *IEEE Trans. Power Electron.*, vol. 33, no. 5, pp. 4088–4101, May 2018.

[4] R. Gomez-Merchan, S. Vazquez, A. Marquez Alcaide, H. Dehghani Tafti, J. I. Leon, J. Pou, C. A. Rojas, S. Kouro, and L. G. Franquelo, "Binary search-based flexible power point tracking algorithm for photovoltaic systems," *IEEE Trans. Ind. Electron.*, pp. 1–1, 2020, to be published, 10.1109/TIE.2020.2998743.

[5] C. Y. Tang, Y. T. Chen, and Y. M. Chen, "PV power system with multi-mode operation and low-voltage ride-through capability," *IEEE Trans. Ind. Electron.*, vol. 62, no. 12, pp. 7524–7533, Dec. 2015.

[6] H. D. Tafti, C. D. Townsend, G. Konstantinou, and J. Pou, "A multi-mode flexible power point tracking algorithm for photovoltaic power plants," *IEEE Trans. Power Electron.*, vol. 34, no. 6, pp. 5038–5042, Jun., 2019.

[7] H. D. Tafti, A. Sangwongwanich, Y. Yang, J. Pou, G. Konstantinou, and F. Blaabjerg, "An adaptive control scheme for flexible power point tracking in photovoltaic systems," *IEEE Trans. Power Electron.*, vol. 34, pp. 5451–5463, Jun. 2019.

[8] A. Sangwongwanich, Y. Yang, F. Blaabjerg, and D. Sera, "Delta power control strategy for multistring grid-connected PV inverters," *IEEE Trans. Ind. Appl.*, vol. 53, no. 4, pp. 3862–3870, Jul. 2017.

[9] Y. Yang, E. Koutroulis, A. Sangwongwanich, and F. Blaabjerg, "Pursuing photovoltaic cost-effectiveness: Absolute active power control offers hope in single-phase PV systems," *IEEE Ind. Appl. Mag.*, vol. 23, no. 5, pp. 40–49, Jun. 2017.

[10] H. D. Tafti, A. Sangwongwanich, Y. Yang, G. Konstantinou, J. Pou, and F. Blaabjerg, "A general algorithm for flexible active power control of photovoltaic systems," in *Proc. of APEC*, pp. 1115–1121, Mar. 2018.